Front. Energy 2017, 11(1): 85–91
DOI 10.1007/s11708-016-0437-3

RESEARCH ARTICLE

**Lei ZHAO, Wenbin ZHANG, Jingwei CHEN, Hongwei DIAO, Qi WANG, Wenjing WANG**

# Plasma enhanced chemical vapor deposition of excellent a-Si:H passivation layers for a-Si:H/c-Si heterojunction solar cells at high pressure and high power

© Higher Education Press and Springer-Verlag Berlin Heidelberg 2016

**Abstract** The intrinsic a-Si:H passivation layer inserted between the doped a-Si:H layer and the c-Si substrate is very crucial for improving the performance of the a-Si:H/c-Si heterojunction (SHJ) solar cell. The passivation performance of the a-Si:H layer is strongly dependent on its microstructure. Usually, the compact a-Si:H deposited near the transition from the amorphous phase to the nanocrystalline phase by plasma enhanced chemical vapor deposition (PECVD) can provide excellent passivation. However, at the low deposition pressure and low deposition power, such an a-Si:H layer can be only prepared in a narrow region. The deposition condition must be controlled very carefully. In this paper, intrinsic a-Si:H layers were prepared on n-type Cz c-Si substrates by 27.12 MHz PECVD at a high deposition pressure and high deposition power. The corresponding passivation performance on c-Si was investigated by minority carrier lifetime measurement. It was found that an excellent a-Si:H passivation layer could be obtained in a very wide deposition pressure and power region. Such wide process window would be very beneficial for improving the uniformity and the yield for the solar cell fabrication. The a-Si:H layer microstructure was further investigated by Raman and Fourier transform infrared (FTIR) spectroscopy characterization. The correlation between the microstructure and the passivation performance was revealed. According to the above findings, the a-Si:H passivation performance was optimized more elaborately. Finally, a large-area SHJ solar cell with an efficiency of 22.25% was fabricated on the commercial 156 mm pseudo-square n-type Cz c-Si substrate with the open-circuit voltage ($V_{oc}$) of up to 0.732 V.

**Keywords** PECVD, high pressure and high power, a-Si:H microstructure, passivation, heterojunction solar cell

Received August 6, 2016; accepted October 10, 2016

Lei ZHAO, Wenjing WANG
Key Laboratory of Solar Thermal Energy and Photovoltaic System of Chinese Academy of Sciences, Institute of Electrical Engineering, Chinese Academy of Sciences, Beijing 100190, China; University of Chinese Academy of Sciences, Beijing 100049, China

Jingwei CHEN, Hongwei DIAO
Key Laboratory of Solar Thermal Energy and Photovoltaic System of Chinese Academy of Sciences, Institute of Electrical Engineering, Chinese Academy of Sciences, Beijing 100190, China

Wenbin ZHANG, Qi WANG (✉)
GCL System Integration Technology Co. Ltd, Shanghai 201406, China
E-mail: wangqi1@gclsi.com

## 1 Introduction

Amorphous/crystalline silicon (a-Si:H/c-Si) heterojunction (SHJ) solar cell has attracted a great deal of attention for photovoltaic applications [1–4]. The surface passivation of c-Si is of critical importance for the SHJ solar cell to achieve high efficiency. One representative of the SHJ solar cell is the so-called HIT (heterojunction with intrinsic thin-layer) cell proposed by Sanyo Ltd [1]. An intrinsic a-Si:H thin layer is inserted between the doped a-Si:H layer and the c-Si substrate to passivate the interface. The wide bandgap ($E_g$) of the doped a-Si:H emitter, together with the excellent passivation performance given by the thin intrinsic a-Si:H layer, endows the solar cell very high open-circuit voltage ($V_{OC}$) and conversion efficiency ($\eta$). By using this technology, Panasonic has achieved a record $\eta$ of 24.7% with a $V_{OC}$ value of up to 750 mV [4]. It is well known that a-Si:H can be prepared by several deposition techniques, such as plasma enhanced chemical vapor deposition (PECVD) [5], hot wire chemical vapor deposition (HWCVD) [6]. PECVD has been established for industrial application. Many researchers have studied the impact of some deposition parameters of PECVD on the a-Si:H passivation performance, such as plasma frequency [7], substrate temperature [8], hydrogen dilution ratio [9],

deposition pressure [10], $H_2$ plasma exposure [11]. Different deposition conditions resulted in different passivation performances. The deposition condition can change the deposited film microstructure, especially the hydrogen distribution inside the film, which is closely related to the passivation performance. It has been found that a-Si:H has a better passivation effect due to its relatively higher hydrogen content compared with microcrystalline silicon (μc-Si) or nanocrystalline silicon (nc-Si) while hydrogen atoms in the form of Si-H bonds are more preferred to those in the form of Si-H2 bonds [12]. Meddeb et al. studied the effect of hydrogen dilution on passivation [13]. They have found that at lower hydrogen dilution rates ($R < 2$), the polymerization reaction of silane molecules in the plasma bulk as well as the excess of dihydride (Si-H2) incorporation in the as-deposited layers results in higher microvoid density and worse passivation quality. In contrast, the deposition at higher hydrogen dilution rates ($R > 5$) leads to the degradation of the film quality with very low hydrogen content and crystalline epitaxial growth at the a-Si/c-Si interface. Thus, the best material quality is obtained just below the onset of amorphous to crystalline transition ($R = 3$). Zhang et al. have also presented that a-Si:H with a high passivation performance should be deposited prior to the formation of amorphous-to-nanocrystalline transition phase [14]. In order to obtain the above a-Si:H passivation layer, the deposition at low pressure and low power for PECVD is usually adopted. Kim et al. have shown that the deposition pressure should be controlled at about 80–110 Pa [10]. For the deposition pressure, Ge et al. have also proposed a narrow range of 60–75 Pa [15]. Guo et al. have suggested that the ratio of the deposition power to pressure ($C_{pp}$ in W/Pa) should be in the range of 0.75–1.25 [16]. All the results indicate that the process window to achieve an excellent a-Si:H passivation layer is narrow if the deposition is performed at a low pressure and low power. So the deposition condition should be maintained strictly, or the uniformity and the yield cannot be effectively guaranteed. In this paper, the deposition at a high pressure and high power was investigated to widen the process window. Meanwhile, the correlation between the a-Si:H microstructure and its passivation performance was also checked in this case.

## 2 Experimental

A deposition pressure series and a deposition power series of the intrinsic a-Si:H layers were deposited by a 27.12 MHz PECVD system at 200°C with a gas flow rate ratio $[SiH_4]:[H_2]$ of 1:3. For the pressure series, the deposition power was fixed at 300 W and the pressure was varied from 133 Pa to 665 Pa. For the power series, the deposition pressure was fixed at 399 Pa and the power was varied from 100 W to 900 W. To check the passivation performance, the a-Si:H layers were deposited on both sides of n-type Cz c-Si substrates. It was well known that the a-Si:H passivation performance was dependent on its thickness [17]. Deligiannis et al. reported that the a-Si:H passivation performance could be improved as its thickness increased gradually. When the thickness was up to 29 nm, the passivation performance was almost saturated, and not affected by the thickness increase again [18]. In this paper, the a-Si:H thickness was controlled at about 50 nm. Thus the thickness dependence of the passivation performance could be excluded. The c-Si substrates had a thickness of about 180 μm. Before the deposition, the c-Si substrates were chemically polished in an aqueous NaOH solution of about 20% to remove the raw damaged surface. Then, the standard RCA cleaning processes were conducted, followed by the dipping of several minutes in a dilute HF solution of 1% to remove the native oxide. After the deposition, a specific post annealing treatment was performed to promote the passivation effect. Then the passivation performance was checked by measuring the effective minority carrier lifetime via WCT-120 Sinton. Further, another relatively thicker layer deposited on c-Si substrate was prepared for Fourier transform infrared spectroscopy (FTIR) measurement to investigate the hydrogen distribution inside the film via the Varian 3100 Excalibur system. In order to reveal the crystalline state by Raman characterization, the corresponding layers were also deposited on quartz substrates. Before the deposition, the quartz substrates were degreased, in turn, by acetone, alcohol, and DI water cleaning, and were finally dipped in the dilute HF solution. Raman measurement was performed via the LabRAM HR system from HORIBA Scientific. The laser wavelength was 488 nm and a low power of 10 mW was adopted.

For the SHJ solar cell fabrication, the p-type and n-type doping for a-Si:H layers were realized by incorporating $B_2H_6$ and $PH_3$ into the $SiH_4:H_2$ plasma, respectively. The c-Si substrates were textured in an aqueous NaOH solution of about 2% at about 85°C to form random pyramids on the surface. Transparent conductive oxide (TCO) layers were deposited by reactive plasma deposition (RPD). Ag metal grids were prepared by screen-printing of the low-temperature Ag paste. The final solar cell was Ag/TCO/a-Si:H(p)/a-Si:H(i)/c-Si(n)/a-Si:H(i)/a-Si:H($n^+$)/TCO/Ag. Then the light current-voltage (*I-V*) characteristic of the solar cell was measured under the illumination of an AM1.5 solar simulator from IVT Solar Pte Ltd.

## 3 Results and discussion

The passivation effect of a-Si:H layers was characterized by the effective minority carrier lifetime ($\tau_{eff}$) measurement. Utilizing the $\tau_{eff}$ obtained, the effective surface recombination velocity ($S_{eff}$) can be calculated by Eq. (1) with the assumption that both surfaces have the same

values ($S_{eff} = S_{front} = S_{back}$) as the sample structure is symmetrical [19,20].

$$S_{eff} = \frac{W}{2}\left(\frac{1}{\tau_{eff}} - \frac{1}{\tau_b}\right), \quad (1)$$

where $\tau_b$ is the bulk recombination lifetime and $W$ is the wafer thickness. The uncertainty of $S_{eff}$ depends on the $\tau_b$ value used. When $\tau_b$ is assumed to be infinite, the maximum limit of the effective surface recombination velocity ($S_{eff,max}$) can be achieved.

The $\tau_{eff}$ and $S_{eff,max}$ obtained as functions of the deposition pressure and power are shown in Fig. 1. When the deposition pressure increases from 133 to 532 Pa, $\tau_{eff}$ increases significantly from 0.54 to 4.3 ms. $S_{eff,max}$ can be as low as 2.3 cm/s. As the deposition pressure increases further, $\tau_{eff}$ decreases inversely. However, it can be clearly seen that a $\tau_{eff}$ higher than 3 ms and a $S_{eff,max}$ lower than 3 cm/s can be achieved when the deposition pressure is in a wide range from approximately 400 to 600 Pa. When the deposition pressure is fixed at 399 Pa and the deposition power is changed from 100 to 900 W, similar trends are observed for $\tau_{eff}$ and $S_{eff,max}$. A high $\tau_{eff}$ and a low $S_{eff,max}$ can be achieved when the deposition power is in a wide range from about 600 to 800 W. The results show that an excellent a-Si:H passivation layer can be fabricated in a wide deposition pressure and power region when the high pressure and high power deposition is adopted. Thus, a wide process window for the SHJ solar cell fabrication can be provided, which will be very beneficial for improving the uniformity and the yield of the solar cells.

Obviously, the passivation performance is related to the a-Si:H microstructure. Generally, the silicon thin film deposited by PECVD can be considered as a mixture material of amorphous phase, crystalline phase, and interface phase. The Raman spectrum of the amorphous phase consists of four distinct bands at about 150 cm$^{-1}$, 307 cm$^{-1}$, 423 cm$^{-1}$ and 480 cm$^{-1}$, associated with Si-Si transverse acoustic (TA), longitudinal acoustic (LA), longitudinal optic (LO) and transverse optic (TO) vibrational modes [21,22]. For the crystalline phase, the Si-Si TO mode will move to 520 cm$^{-1}$. The corresponding mode of interface phase exists between 480 and 520 cm$^{-1}$. Therefore, the TO mode for a specific silicon thin film is a scattering sum of the above three phases and thus can be resolved into three Gaussian curves. Then, the film microstructure can be deduced by the positions and intensities of the corresponding Gaussian peaks [12]. Figure 2 depicts the Raman spectra of the deposited a-Si:H layers. The fact that the Si-Si TO mode occurs at about 480 cm$^{-1}$ illustrates that all the layers are mainly composed of the amorphous phase.

Furthermore, FTIR is utilized to investigate the hydrogen distribution inside the films as demonstrated in Fig. 3. For the silicon thin films, the absorption peaks in the range of 1900 to 2200 cm$^{-1}$ correspond to the stretching modes, which can be decomposed into two Gaussians to determine the contribution of Si-H mono-hydrides (about 2000 cm$^{-1}$ ) and Si-H2 clusters (about 2100 cm$^{-1}$) inside the films. The microstructure parameter ($R^*$) is utilized as the indicator to evaluate the film microstructure quality [23].

$$R^* = \frac{I_{2100}}{I_{2000} + I_{2100}}, \quad (2)$$

where $I_{2000}$ and $I_{2100}$ are the integrated absorption intensities at about 2000 and 2100 cm$^{-1}$, respectively. As shown in Fig. 3, when the deposition pressure or power increases gradually, the main peak of FTIR fundamentally moves from $I_{2100}$ to $I_{2000}$ first and then returns to $I_{2100}$ again. The corresponding $R^*$ values are further displayed in Fig. 4. Clearly, at an appropriate high pressure and high power, the lowest $R^*$ is achieved. The low $R^*$ means that the H atoms in the a-Si:H matrix mainly exist in the Si-H form. The low intensity of Si-H2 bonds indicates that the

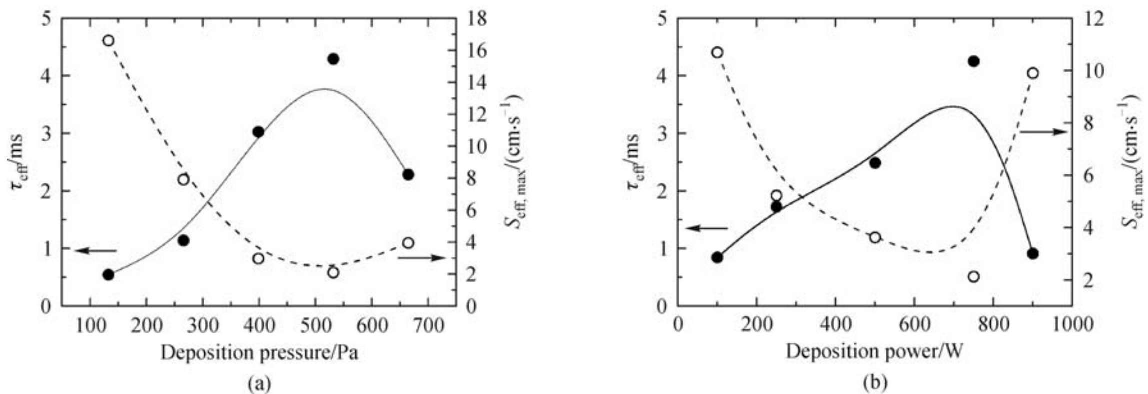


**Fig. 1** Effective minority carrier lifetime ($\tau_{eff}$) and maximum limit of effective surface recombination velocity ($S_{eff,max}$) obtained via a-Si:H passivation layers deposited at different conditions

(a) Deposition power is 300 W and deposition pressure is varied from 133 to 665 Pa; (b) deposition pressure is 399 Pa and deposition power is varied from 100 to 900 W

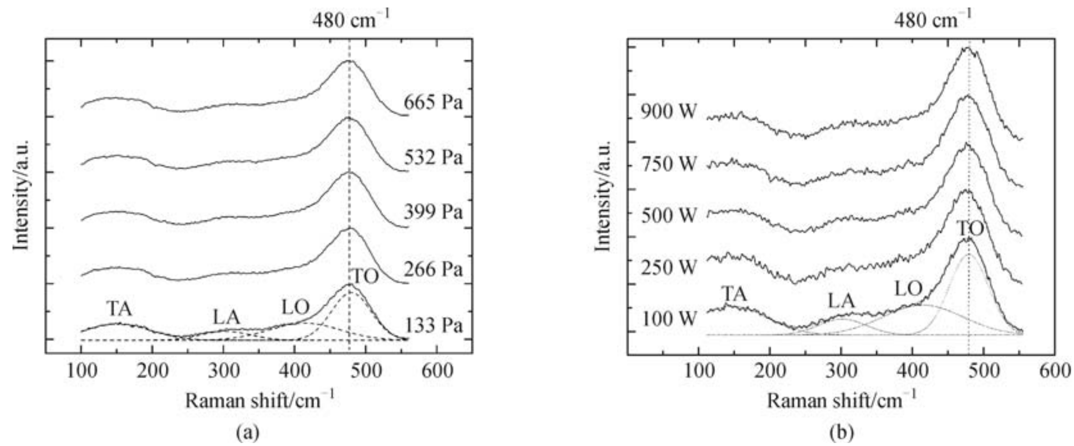


**Fig. 2** Raman spectra of the a-Si:H thin films deposited on the quartz substrates at different conditions
(a) Deposition power is 300 W and deposition pressure is varied from 133 to 665 Pa; (b) deposition pressure is 399 Pa and deposition power is varied from 100 W to 900 W

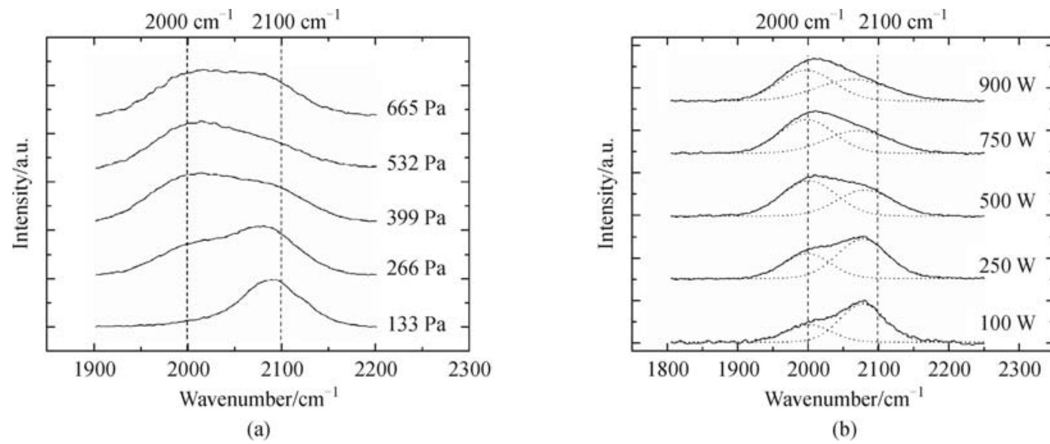


**Fig. 3** FTIR spectra of the a-Si:H thin films deposited on the c-Si substrates at different conditions
(a) Deposition power is 300 W and deposition pressure is varied from 133 to 665 Pa; (b) deposition pressure is 399 Pa and deposition power is varied from 100 to 900 W

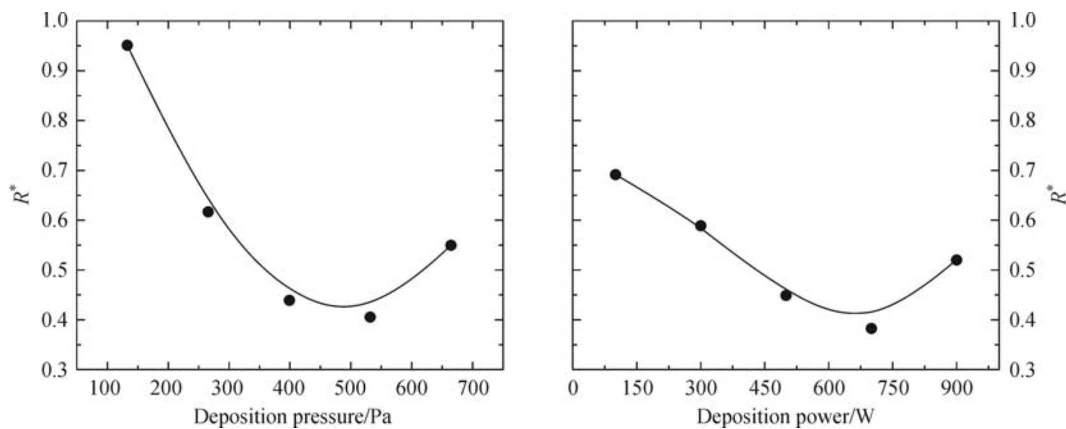


**Fig. 4** Microstructure parameter ($R^*$) of a-Si:H thin films obtained according to FTIR spectra

a-Si:H film has a compact microstructure with few voids and crystallites inside, which is well present in Fig. 5 by a representative transmission electron microscopy (TEM) photograph.

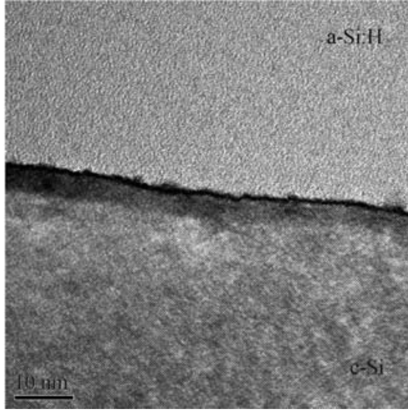


**Fig. 5** Representative transmission electron microscopy (TEM) photograph for obtained compact a-Si:H layer on c-Si substrate

When the deposition power/pressure is low/high, the decomposition efficiency of $SH_4$ is not efficient. The bonding structure is mainly Si-H2, which results in a defective material with a high void density. The increase/decrease of the deposition power/pressure is expected to improve the decomposition efficiency of $SiH_4$ gradually, and meanwhile, the weak bonding structure can be etched off by the atomic H with the increased energy in the gas phase. Therefore, the main H bonding changes from Si-H2 to Si-H, resulting in the gradual decrease of the microstructure parameter $R^*$. However, when the deposition power/pressure is over high/low, the ion bombardment will induce Si-H2 defects into the deposited film again. $R^*$ increases reversely. Thus, the lowest $R^*$ can be obtained at an appropriate combination of the deposition power and pressure.

By comparing Figs. 1 and 4, the correlation between the microstructure parameter $R^*$ and the lifetime $\tau_{\text{eff}}$ can be seen apparently. The reduction of $R^*$ results in the increase of $\tau_{\text{eff}}$. The compact a-Si:H with hydrogen atoms preferring to form monohydrides, instead of dihydrides, has the excellent passivation performance on the c-Si surface. It should be noted that the lowest $R^*$ obtained here is still high (up to about 0.4). A further reduction of $R^*$ can make a-Si:H more compact. However, high bulk quality of a-Si:H layers with over dense structures may have low hydrogen content ($C_{\text{H}}$). To have good passivation performance, sufficient hydrogen atoms must be provided from the a-Si:H passivation layers to saturate the dangling bonds on the a-Si:H/c-Si interface. Guo et al. demonstrated that the passivation performance was strongly governed by $C_{\text{H}}$, which should be in the range of 5.0% to 8.5% [24]. Therefore, $C_{\text{H}}$ was further calculated for the deposition power series according to the FTIR absorption via [25]

$$C_{\text{H}} = \frac{A_{2000}I_{2000}}{N_{\text{Si}}} + \frac{A_{2100}I_{2100}}{N_{\text{Si}}}, \tag{3}$$

where the proportionality constants $A_{2000} = 9.0 \times 10^{19}$ cm$^{-2}$ and $A_{2100} = 2.2 \times 10^{20}$ cm$^{-2}$. The density of silicon $N_{\text{Si}} = 5.0 \times 10^{22}$ cm$^{-3}$. $I_{2000}$ and $I_{2100}$ are the integrated intensities at about 2000 and 2100 cm$^{-1}$ respectively via

$$I = \int_{\omega_1}^{\omega_2} \frac{\alpha(\omega)}{\omega} \mathrm{d}\omega, \tag{4}$$

where $\alpha$ is the infrared absorption coefficient. $\omega$ is the oscillator frequency. The obtained $C_{\text{H}}$ is shown in Fig. 6. When the deposition power is from 600 W to 800 W, $\tau_{\text{eff}}$ is higher than 3 ms and $C_{\text{H}}$ is about 7.0% (at.). The results illustrate that it is relatively easy to get the compact a-Si:H material with sufficient hydrogen content for the excellent passivation when the high pressure and high power deposition is adopted.

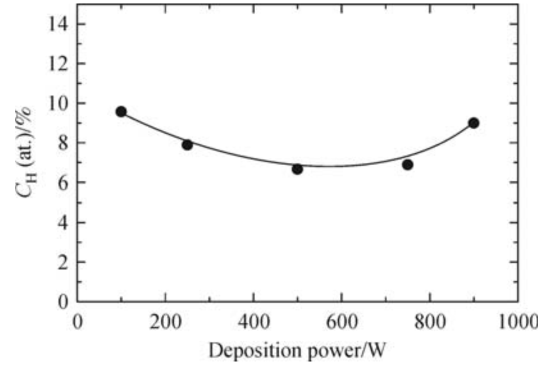


**Fig. 6** Hydrogen content ($C_{\text{H}}$) in a-Si:H films deposited at a pressure of 399 Pa with power varied from 100 to 900 W

Based on the above findings, the deposition condition was further optimized at high deposition power and high deposition pressure. With the optimized a-Si:H passivation layer, the highest minority carrier lifetime $\tau_{\text{eff}} = 9.3$ ms was achieved at $\Delta n = 10^{15}$ cm$^{-3}$, as exhibited in Fig. 7. Then, the complete solar cell fabrication process was optimized systematically. As a result, an excellent SHJ solar cell with an efficiency of 22.25% was achieved successfully on the commercial 156 mm pseudo-square n-type Cz c-Si substrate. As shown in Fig. 8, the solar cell $V_{\text{oc}}$ is up to 0.732 V, which indicates that a very excellent passivation performance is realized.

## 4 Conclusions

The correlation was investigated between the microstructure and the passivation performance of the intrinsic a-Si:H layer on the c-Si substrate by preparing the a-Si:H layers at high deposition pressure and high deposition power by 27.12 MHz plasma enhanced chemical vapor deposition (PECVD). It was found that in the high pressure and high

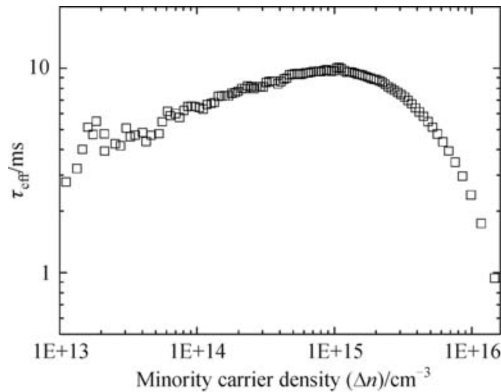


**Fig. 7** Highest effective minority carrier lifetime ($\tau_{eff}$) achieved by optimized deposition condition at a relatively high pressure and high power

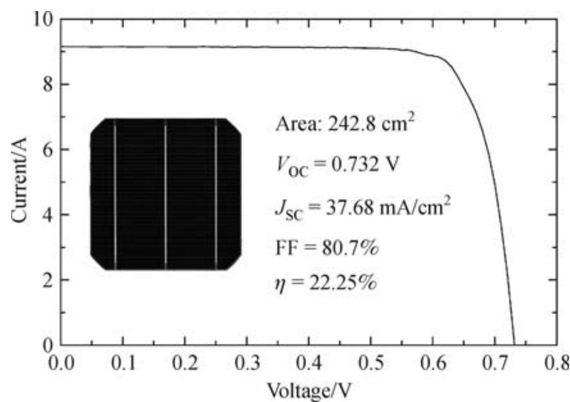


**Fig. 8** Light current-voltage (*I-V*) performance of optimized a-Si:H/c-Si heterojunction (SHJ) solar cell obtained on commercial 156 mm pseudo-square n-type Cz c-Si substrate

power region, the compact a-Si:H with sufficient hydrogen content and most of hydrogen atoms in the form of monohydrides could be prepared to realize excellent passivation performance in a wide pressure and power range, which would provide a wide process window for the a-Si:H/c-Si heterojunction (SHJ) solar cell fabrication and thus improve the uniformity and the yield of the fabricated solar cells. As a demonstration, a large-area SHJ solar cell with an efficiency of 22.25% was fabricated on the commercial 156 mm pseudo-square n-type Cz c-Si substrate with an open-circuit voltage ($V_{oc}$) of up to 0.732 V. Therefore, preparation of the a-Si:H passivation layer at a high pressure and high power via PECVD has a great potential for the mass production of the SHJ solar cell.

**Acknowledgements** This work was supported by the National High Technology Research and Development Program of China (863 Program) (Grant No. 2011AA050502) and the National Natural Science Foundation of China (Grant No. 61274061).

## References

1. Taguchi M, Tanaka M, Matsuyama T, Matsuoka T, Tsuda S, Nakano S, Kishi Y, Kuwano Y. Improvement of the conversion efficiency of polycrystalline silicon thin film solar cell. In: Proceedings of Technical Digest of the 5th International Photovoltaic Science and Engineering Conference. Kyoto, Japan, 1990: 689–692
2. Scherg-Kurmes H, Körner S, Ring S, Klaus M, Korte L, Ruske F, Schlatmann R, Rech B, Szyszka B. High mobility $In_2O_3$:H as contact layer for a-Si:H/c-Si heterojunction and c-Si:H thin film solar cells. Thin Solid Films, 2015, 594: 316–322
3. Taguchi M, Yano A, Tohoda S, Matsuyama K, Nakamura Y, Nishiwaki T, Fujita K, Maruyama E. 24.7% record efficiency HIT solar cell on thin silicon wafer. IEEE Journal of Photovoltaics, 2014, 4(1): 96–99
4. de Wolf S, Descoeudres A, Holman Z C, Ballif C. High-efficiency silicon heterojunction solar cells: a review. Green, 2012, 2(1): 7–24
5. Schulze T F, Korte L, Rech B. Impact of a-Si:H hydrogen depth profiles on passivation properties in a-Si:H/c-Si heterojunctions. Thin Solid Films, 2012, 520(13): 4439–4444
6. Wang Q, Page M R, Iwaniczko E, Xu Y Q, Roybal L, Bauer R, To B, Yuan H C, Duda A, Hasoon F, Yan Y F, Levi D, Meier D, Branz H M, Wang T H. Efficient heterojunction solar cells on p-type crystal silicon wafers. Applied Physics Letters, 2010, 96(1): 013507
7. Fesquet L, Olibet S, Vallat-Sauvain E, Shah A, Ballif C. High quality surface passivation and heterojunction fabrication by VHF-PECVD deposition of amorphous silicon on crystalline Si: theory and experiments. In: Proceedings of 23rd European Photovoltaic Solar Energy Conference and Exhibition. Valencia, Spain, 2008, 2: 2DV 2.14
8. Fujiwara H, Kaneko T, Kondo M. Optimization of interface structures in crystalline silicon heterojunction solar cells. Solar Energy Materials and Solar Cells, 2009, 93(6-7): 725–728
9. Kim S K, Lee J C, Park S J, Kim Y J, Yoon K H. Effect of hydrogen dilution on intrinsic a-Si:H layer between emitter and Si wafer in silicon heterojunction solar cell. Solar Energy Materials and Solar Cells, 2008, 92(3): 298–301
10. Kim S, Dao V A, Shin C, Cho J, Lee Y, Balaji N, Ahn S, Kim Y, Yi J. Low defect interface study of intrinsic layer for c-Si surface passivation in a-Si:H/c-Si heterojunction solar cells. Thin Solid Films, 2012, 521: 45–49
11. Lee S J, Kim S H, Kim D W, Kim K H, Kim B K, Jang J. Effect of hydrogen plasma passivation on performance of HIT solar cells. Solar Energy Materials and Solar Cells, 2011, 95(1): 81–83
12. Zhao L, Diao H W, Zeng X B, Zhou C L, Li H L, Wang W J. Comparative study of the surface passivation on crystalline silicon by silicon thin films with different structures. Physica B: Condensed Matter, 2010, 405(1): 61–64
13. Meddeb H, Bearda T, Abdelraheem Y, Ezzaouia H, Gordon I, Szlufcik J, Poortmans J. Structural, hydrogen bonding and in situ studies of the effect of hydrogen dilution on the passivation by amorphous silicon of n-type crystalline (100) silicon surfaces. Journal of Physics D: Applied Physics, 2015, 48(41): 415301
14. Zhang L P, Liu W Z, Guo W W, Bao J, Zhang X Y, Liu J N, Wang D

L, Meng F Y, Liu Z X. Interface processing of amorphous-crystalline silicon heterojunction prior to the formation of amorphous-to-nanocrystalline transition phase. IEEE Journal of Photovoltaics, 2016, 6(3): 604–610

15. Ge J, Ling Z P, Wong J, Stangl R, Aberle A G, Mueller T. Analysis of intrinsic hydrogenated amorphous silicon passivation layer growth for use in heterojunction silicon wafer solar cells by optical emission spectroscopy. Journal of Applied Physics, 2013, 113(23): 234310
16. Guo W W, Zhang L P, Bao J, Meng F Y, Liu J N, Wang D L, Bian J Y, Liu W Z, Feng Z Q, Verlinden P J, Liu Z X. Defining a parameter of plasma-enhanced CVD to characterize the effect of silicon-surface passivation in heterojunction solar cells. Japanese Journal of Applied Physics, 2015, 54(4): 041402
17. Geissbühler J, De Wolf S, Demaurex B, Seif J P, Alexander D T L, Barraud L, Ballif C. Amorphous/crystalline silicon interface defects induced by hydrogen plasma treatments. Applied Physics Letters, 2013, 102(23): 231604
18. Deligiannis D, Marioleas V, Vasudevan R, Visser C C G, van Swaaij R A C M M, Zeman M. Understanding the thickness-dependent effective lifetime of crystalline silicon passivated with a thin layer of intrinsic hydrogenated amorphous silicon using a nanometer-accurate wet-etching method. Journal of Applied Physics, 2016, 119(23): 235307
19. De Wolf S. Intrinsic and doped a-Si:H/c-Si interface passivation. In: Physics and Technology of Amorphous-crystalline Heterostructure Silicon Solar Cells. Berlin: Springer-Verlag Berlin Heidelberg, 2012: 223–259
20. Sproul A B. Dimensionless solution of the equation describing the effect of surface recombination on carrier decay in semiconductors. Journal of Applied Physics, 1994, 76(5): 2851–2854
21. Beeman D, Tsu R, Thorpe M F. Structural information from the Raman spectrum of amorphous silicon. Physical Review B: Condensed Matter and Materials Physics, 1985, 32(2): 874–878
22. Morell G, Katiyar R S, Weisz S Z, Jia H, Shinar J, Balberg I. Raman study of the network disorder in sputtered and glow discharge a-Si:H films. Journal of Applied Physics, 1995, 78(8): 5120–5125
23. Ouwens J D, Schropp R E I. Hydrogen microstructure in hydrogenated amorphous silicon. Physical Review B: Condensed Matter and Materials Physics, 1996, 54(24): 17759–17762
24. Guo W W, Zhang L P, Meng F Y, Bao J, Wang D L, Liu J N, Feng Z Q, Verlinden P J, Liu Z X. Study of the correlation between hydrogenated amorphous silicon microstructure and crystalline silicon surface passivation in heterojunction solar cells. Physica Status Solidi A: Applications and Materials Science, 2015, 212(10): 2233–2238
25. Langford A A, Fleet M L, Nelson B P, Lanford W A, Maley N. Infrared absorption strength and hydrogen content of hydrogenated amorphous silicon. Physical Review B: Condensed Matter and Materials Physics, 1992, 45(23): 13367–13377